

A quantitative structure comparison with persistent similarity

Kelin Xia^{1,2} *

¹Division of Mathematical Sciences, School of Physical and Mathematical Sciences,
Nanyang Technological University, Singapore 637371

²School of Biological Sciences, Nanyang Technological University, Singapore 637371

August 27, 2018

Abstract

Biomolecular structure comparison not only reveals evolutionary relationships, but also sheds light on biological functional properties. However, traditional definitions of structure or sequence similarity always involve superposition or alignment and are computationally inefficient. In this paper, I propose a new method called persistent similarity, which is based on a newly-invented method in algebraic topology, known as persistent homology. Different from all previous topological methods, persistent homology is able to embed a geometric measurement into topological invariants, thus provides a bridge between geometry and topology. Further, with the proposed persistent Betti function (PBF), topological information derived from the persistent homology analysis can be uniquely represented by a series of continuous one-dimensional (1D) functions. In this way, any complicated biomolecular structure can be reduced to several simple 1D PBFs for comparison. Persistent similarity is then defined as the quotient of sizes of intersect areas and union areas between two correspondingly PBFs. If structures have no significant topological properties, a pseudo-barcode is introduced to insure a better comparison. Moreover, a multiscale biomolecular representation is introduced through the multiscale rigidity function. It naturally induces a multiscale persistent similarity. The multiscale persistent similarity enables an objective-oriented comparison. State differently, it facilitates the comparison of structures in any particular scale of interest. Finally, the proposed method is validated by four different cases. It is found that the persistent similarity can be used to describe the intrinsic similarities and differences between the structures very well.

Key words: Protein structure, Topology, Persistent homology, Betti number, Barcodes, Persistent similarity, Persistent Betti function (PBF), Multiscale persistent homology

*Address correspondences to Kelin Xia. E-mail:xiakelin@ntu.edu.sg

Contents

1	Introduction	3
2	Methodology	4
2.1	Persistent homology	5
	Simplicial complex	5
	Homology	6
	Rips complex	6
	Filtration	7
	Persistent homology	7
2.2	Persistent similarity	7
	Persistent Betti function (PBF)	8
	Persistent similarity	8
2.3	Multiscale persistent similarity	9
	Multiscale rigidity function	9
	Multiscale persistent homology	9
	Multiscale persistent similarity	9
3	Results and discussion	10
3.1	Case 1: Two similar nucleotide kinases	10
3.2	Case 2: NMR configurations	12
3.3	Case 3: Steered dynamic simulation	14
3.4	Case 4: Fullerene C_{44} isomers	15
4	Conclusion remarks	17

1 Introduction

The most prominent feature of biological sciences in the 21st century is its transition from an empirical, qualitative and phenomenological discipline to a comprehensive, quantitative and predictive one. With the accumulation of gigantic structure and sequence data in Protein Data Bank, Gene Bank, and protein structure classification databanks CATH and SCOP, revolutionary opportunities have arisen for data-driven advances in biological research. An essential component of quantitative biology is geometric analysis. Geometric measurements, algorithms and modeling offer a basis for molecular visualization, bridge the gap between experimental data from X-ray, NMR, and Cryo-electron microscopy, and theoretical models, and play a fundamental role in the analysis of biomolecular structure, function, dynamics, and transport. Especially with the aid from increasingly powerful high performance computers, geometric analysis becomes more and more deeply involved in biological sciences. However, geometric invariants usually describe local features, such as distances, angles, curvatures, convexity, etc. As a consequence, geometric analysis tends to involve excessive irrelevant structure details and become computationally intractable, especially for macromolecules and protein complexes. Great promises come from a newly founded area in big data analysis, known as topological data analysis (TDA). The essence of TDA is to employ concepts and algorithms from algebraic topology and computational topology to extract or identify intrinsic properties of the data. These intrinsic properties are topological invariants, which describe global features of the structure and are consistent under continuous deformation.

One of the most important tool in TAD is persistent homology, which is a multiscale representation of topological features.^{13,59,60} Different from the traditional topological method, persistent homology is able to embed a geometric measurement into topological invariants, thus provides a bridge between geometry and topology. To achieve this, a filtration process is employed in persistent homology. Through the systematical variation of filtration value, a series of continuous topological spaces are generated. Topological invariants like connected components, circles, rings, void and cavities are generated. Their lifespans or persistent times are measured and used as geometric measurements of these topological properties. Historically, the general form of persistent homology is proposed by Robins,⁴¹ Edelsbrunner et al.,¹³ and Zomorodian and Carlsson,⁵⁹ independently. Various softwares, including JavaPlex,⁴⁵ Perseus,³³ DIPA,² Dionysus,¹ jHoles,⁴ etc, have been proposed,^{6,9,10,12,31} together with visualization methods, including persistent diagram,³¹ persistent barcode,¹⁹ and persistent landscape.⁵ As a method deeply rooted in algebraic topology, persistent homology has demonstrates great potential in data simplification and complexity reduction.^{13,59} It provides new opportunities for researchers from mathematics, computer sciences, computational biology, biomathematics, engineering, etc. Persistent homology has been used in a variety of fields, including shape recognition,¹¹ network structure,^{21,25,43} image analysis,^{3,8,16,39,44} data analysis,^{7,27,35,40,46} chaotic dynamics verification,^{22,30} computer vision⁴⁴ and computational biology.^{17,23,58}

Recently, persistent homology has been used in analyzing fullerene molecules, proteins, DNAs and various other biomolecules.^{47,48,52} To quantitatively analyze the biomolecular structures and functions, I have proposed the concept of topological fingerprint, which is defined as the consistent pattern within the barcode that has particular structure implications.⁵² Further, I have introduced a multiresolution and multidimensional persistent homology.^{54,55} With the incorporation of a resolution/scale parameter into a specially designed rigidity function, I can deliver a multiscale structure representation that is able to focus on any scale of interest. More importantly, the corresponding persistent homology analysis provides topological information from various scales, and is proved to be very efficient in handling extremely large data from macromolecules or protein complexes. More recently, based on the persistent homology results, I introduce multiscale persistent functions for biomolecular structure characterization.⁴⁹ The essential idea is to combine the multiscale rigidity functions with persistent homology analysis, so as to construct a series of multiscale persistent functions, particularly multiscale persistent entropies, for structure characterization and comparison. My method has been successfully used in protein classification test.⁴⁹ All these previous results have demonstrated the great potential of topological analysis, especially persistent homology analysis, in biomolecule structure analysis. In this paper, I further propose a persistent similarity for a quantitative comparison between different structures. My persistent similarity is based on the persistent Betti function (PBF), one type of the persistent functions proposed in my previous work. Different from all the previous structure similarity definitions, my persistent similarity uses only topological persistence information. In this way, it is free from structure or gene-sequence alignment, thus computationally much more efficient, particularly when many structures are

considered simultaneously.

Biomolecular structure comparison can not only reveal evolutionary relationships, but also provide insights about biological functional properties. Various definitions of structure and sequence similarity are proposed and are widely used in comparison.²⁴ However, all these methods involve superposition or alignment at either global scale or common subregions. Computationally, this process is time-consuming and highly inefficient when many structures are involved. Dramatically different from all these methods, my persistent similarity is based on topological characterization, thus free from structure or sequence alignment. More specifically, for each biomolecular structure, I can generate its topological representation, i.e., a series of barcodes. From these barcodes, I can define unique persistent Betti functions. These are very simply one-dimensional continuous functions defined in exactly the same computational domain. In this way, evaluation of similarity between different structures is transferred into the comparison between one-dimensional functions. More importantly, since each biomolecular structure is associated with a unique barcode representation thus a unique set of one-dimensional PBFs, the comparison among various structures becomes much more efficient, as I only need to deal with similarity of one-dimensional PBFs. More importantly, I have introduced the multiscale persistent similarity, so that the structure comparison can be done in the any particular scale of interest.

It has been noticed that a similar “topological similarity” has been proposed for structure comparison very recently.^{15,28,29} In this model, structure similarity is directly measured from the persistent barcodes, which are generated from persistent homology. Even though the “topological similarities”^{15,28,29} is also based on persistent homology analysis, my persistence similarity differs greatly from it in several aspects. Firstly, I use the previously proposed PBFs.⁴⁹ These PBFs provide a unique representation of persistent barcode. State differently, there is a one to one relation between my PBFs and barcode representations. With these functions, the comparison between different barcodes becomes much more straightforward and efficient. Secondly, a multiscale persistent similarity is defined so that I can systematically compare the structure properties from various scales. Biomolecules, particularly macroproteins or protein complexes, are usually of multiscales ranging from atom, residue, secondary structure, domain, protein monomer, etc. Different topological properties can be found in different scales. And pinpointing to the right scale is of great importance for similarity comparison. In my model, a multiscale rigidity function is employed to represent the structures from various scales. And persistent similarities derived from it capture similarity information in different scales. Thirdly, I introduce a pseudo-barcode to deliver a more precise comparison in the special situation when structures have no significant topological properties. For instance, if a structure has no β_1 barcodes while the others have, topological similarity between this structure and all the others will always be zero, no matter how long or how many β_1 barcodes the others have. This ambiguity is avoided by the introduction of a pseudo-barcode in my persistent similarity. Fourthly, I introduce weight functions and kernel scales in my PBFs. These parameters give us more flexibility in defining the “significance” of the bars. It is found that for some biomolecular functions and properties, only some special barcodes matter while the others are irrelevant. And in this situation, my model can play important role. It should be noticed that I deliberately avoid using the term of “topological similarity”, because “topological similarity” is widely used in network modeling.^{14,26} The term “persistent similarity” captures the essence of the method and is consistent with all previous notations including, persistent homology, persistent Betti number, persistent entropy, etc. Therefore, I believe it is a much better term to use.

The paper is organized as following. Section 2 is devoted for the introduction of the methodology. I will introduce the persistent homology, define the persistent Betti function and propose the persistent similarity. Further, after the introduction of multiscale persistent homology, I will generalize the persistent similarity to multiscale persistent similarity. Section 3 is dedicated to basic results and discussion. Four different cases are studied, including two similar nucleotide kinases, a series of NMR structures, configurations from molecular dynamics simulation and fullerene C_{44} isomers. The paper ends with a conclusion.

2 Methodology

The quantitative analysis of similarities between related three-dimensional biomolecular structures is of great importance to structure biology. The structure relationships not only reveal the biomolecular evolutionary connections, but also help with understanding of biomolecular functional properties and further the development of new and improved materials. Persistent similarity is proposed in the current paper to facilitate an efficient quantitative comparison of biomolecular structures. Since the persistent homology analysis provides

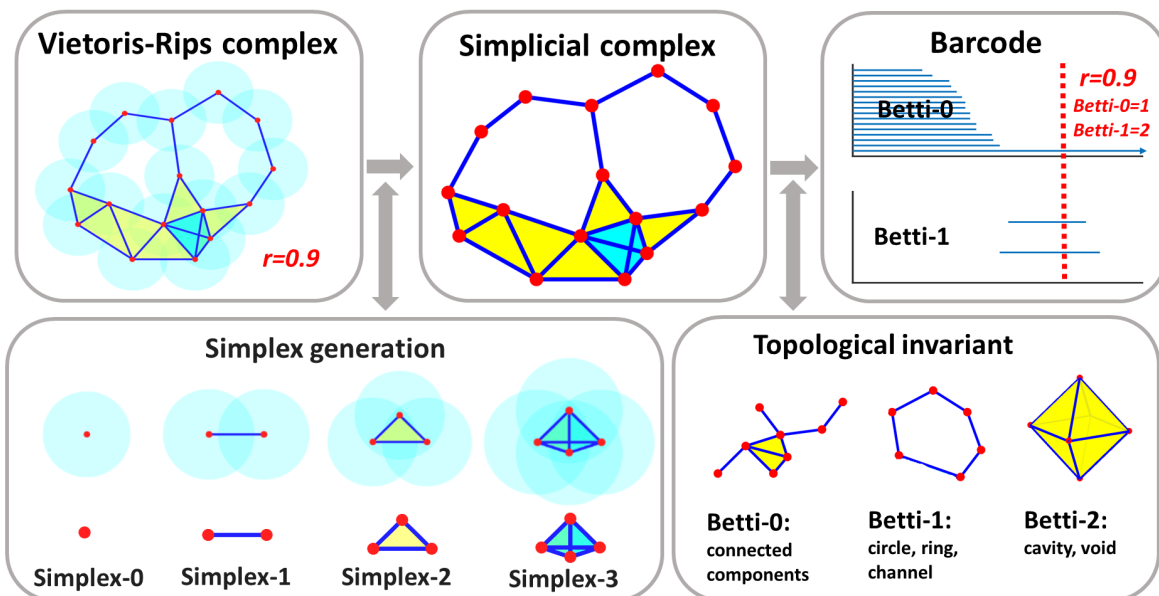


Figure 1: The illustration of the basic concepts in persistent homology analysis. A more general filtration process is demonstrated in Figure 2. The Vietoris-Rips complex is generated with sphere radius equal to 0.9. Its topological information is indicated by the red dash line in the barcode.

a delicate balance between topological simplification and geometric details, the persistent similarity derived from it captures the intrinsic structure properties. To be more specific, the results from the persistent homology analysis are uniquely represented by the proposed persistent Betti functions (PBFs). In this way, the description of biomolecular structures is dramatically simplified into several one-dimensional PBFs. And the comparison of these PBFs results in the persistent similarity. Further, using the multiscale rigidity functions, a multiscale biomolecular representation is delivered and naturally induces a multiscale persistent similarity. A detailed description is given below.

2.1 Persistent homology

Since persistent similarity is derived from persistent homology, a detailed introduction of persistent homology is given in this section. To avoid the heavy mathematical notations and present essential ideas more straightforwardly, I will only focus on the simplicial complex with direct geometric implications. Further, the homology is calculated in Z_2 field and only Vietoris-Rips complex is considered for simplicial complex generation. Interested readers are referred to more detailed description in papers.^{13,59,60}

Simply speaking, homology is a mathematical representation of topological invariants, such as connected components, circle, rings, channels, cavity, void, cage, etc. Persistent homology gives a geometric measurement, i.e., a size, to these invariants. Figure 1 and Figure 2 illustrate the essential concepts used in persistent homology.

Simplicial complex Simplices are the build block for simplicial complex. A set of $k + 1$ affine independent points $v_0, v_1, v_2, \dots, v_k$ can form a k -simplex $\sigma^k = \{v_0, v_1, v_2, \dots, v_k\}$ as following,

$$\sigma^k = \left\{ \lambda_0 v_0 + \lambda_1 v_1 + \dots + \lambda_k v_k \mid \sum_{i=0}^k \lambda_i = 1; 0 \leq \lambda_i \leq 1, i = 0, 1, \dots, k \right\}. \quad (1)$$

Geometrically, a 0-simplex is a vertex, a 1-simplex is an edge, a 2-simplex is a triangle, and a 3-simplex represents a tetrahedron, just as depicted in Figure 1. The i -dimensional face of σ^k is the convex hull formed by $i + 1$ vertices from σ^k ($k > i$). A simplicial complex K is a finite set of simplices that satisfy two essential conditions, i.e., 1) any face of a simplex from K is also in K ; 2) the intersection of any two simplices in K

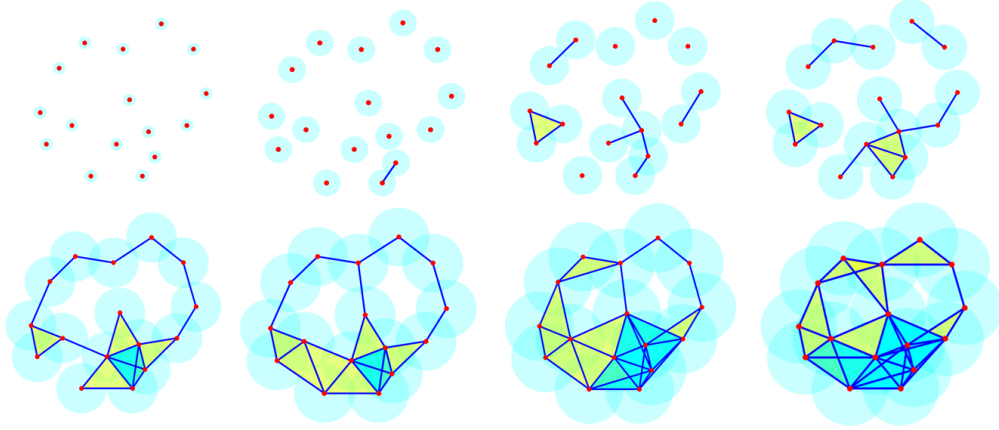


Figure 2: The filtration process and barcode representation of a fullerene C_{60} molecule. During the filtration process, each Carbon atom is associated with a sphere, whose radius increases systematically to generate topologies in various scales. In the molecular barcode representation, each bar represents a homology generator and has unique chemical or physical properties. For β_0 bars, they are related to atom bonds. The ring structures are represented by β_1 bars. The void or cavity structures are captured in β_2 bars.

is either empty or shares faces. Further, we denote an oriented k -simplex as $[\sigma^k]$. An oriented simplex is a simplex together with an orientation, i.e., ordering of its vertex set.

Homology A k -chain c is a linear combination of k -simplexes $c = \sum_i \alpha_i \sigma_i^k$ with $\{\alpha_i \in \mathbb{Z}_2\}$. An Abelian group $C_k(K, \mathbb{Z}_2)$ is formed by the set of all k -chains from the simplicial complex K together with addition operation (modulo-2). A boundary operator ∂_k is defined as $\partial_k : C_k \rightarrow C_{k-1}$. The boundary of an oriented k -simplex $[\sigma^k] = [v_0, v_1, v_2, \dots, v_k]$ can be denoted as,

$$\partial_k[\sigma^k] = \sum_{i=0}^k [v_0, v_1, v_2, \dots, \hat{v}_i, \dots, v_k]. \quad (2)$$

Here $[v_0, v_1, v_2, \dots, \hat{v}_i, \dots, v_k]$ means a $(k-1)$ oriented simplex, which is generated by the elimination of vertex v_i . Further, one has $\partial_0 = 0$ and $\partial_{k-1}\partial_k = 0$. The k -th cycle group Z_k and the k -th boundary group B_k are the subgroups of C_k and can be defined as,

$$Z_k = \text{Ker } \partial_k = \{c \in C_k \mid \partial_k c = 0\}, \quad (3)$$

$$B_k = \text{Im } \partial_{k+1} = \{c \in C_k \mid \exists d \in C_{k+1} : c = \partial_{k+1} d\}. \quad (4)$$

Their elements are called the k -th cycle and the k -th boundary, respectively. It can be noticed that $B_k \subseteq Z_k$, as the boundary of a boundary is always zero $\partial_{k-1}\partial_k = 0$. The k -th homology group H_k is the quotient group generated by the k -th cycle group Z_k and k -th boundary group B_k : $H_k = Z_k/B_k$. The rank of k -th homology group is called k -th Betti number and it can be calculated by

$$\beta_k = \text{rank } H_k = \text{rank } Z_k - \text{rank } B_k. \quad (5)$$

As indicated in Figure 1, the geometric meanings of Betti numbers in \mathbb{R}^3 are as following: β_0 represents the number of isolated components; β_1 is the number of one-dimensional loops, circles, or tunnels; β_2 describes the number of two-dimensional voids or holes. Together, the Betti number sequence $\{\beta_0, \beta_1, \beta_2\}$ describes the intrinsic topological property of the system.

Rips complex For a point set $X \in \mathbb{R}^N$, one defines a cover of closed balls centered at x with radius ϵ . A Rips simplex (or Vietoris-Rips simplex) σ is generated if the largest distance between any of its vertices reaches 2ϵ . Figure 1 illustrates the generation of the Rips simplex.

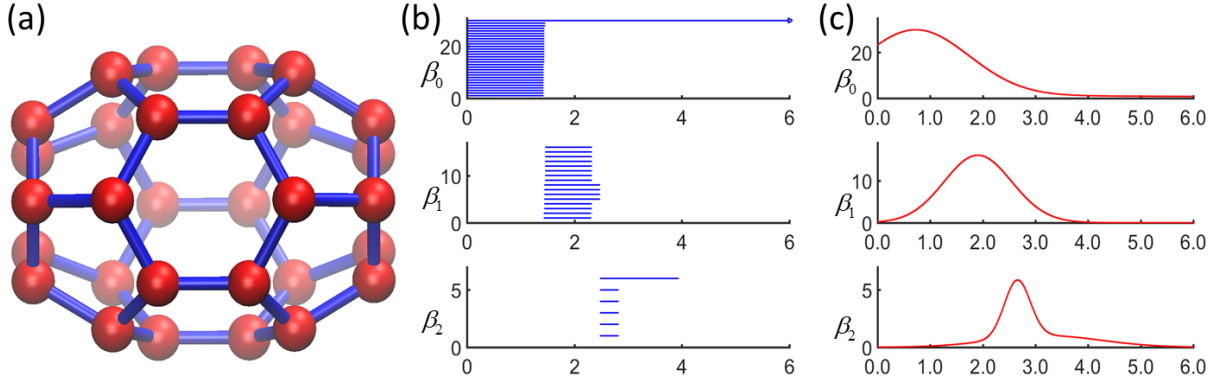


Figure 3: Fullerene C_{44} molecule structure, barcode representation and PBFs. (a) The cage structure of fullerene C_{44} . (b) The barcode representation. Each bar represents a homology generator and has unique chemical or physical properties. For β_0 bars, they are related to atom bonds. The pentagon and hexagon ring structures are represented by β_1 bars. Its cavity or cage structure are captured in β_2 bars. (c) Fullerene C_{44} PBFs.

Filtration In the generation of Rips complex, a radius parameter ϵ is used. However, how to find the best suitable ϵ so that it can best capture the underlying space has been long standing problem. To solve this problem, the idea of filtration has been proposed. As illustrated in Figure 2, instead of finding the best suitable value, an ever-increasing ϵ value is used to generate a series of topological spaces. In this way, the associated topological invariants will have certain “lifespan”, that is some topological invariants last for a wide range of ϵ values, but some invariants disappear very quickly when ϵ value changes.

Persistent homology The filtration can be described as a nested sequence of its subcomplexes,

$$\emptyset = K^0 \subseteq K^1 \subseteq \dots \subseteq K^m = K. \quad (6)$$

And the p -persistent k -th homology group at filtration time i can be represented as

$$H_k^{i,p} = Z_k^i / (B_k^{i+p} \cap Z_k^i). \quad (7)$$

Essentially, persistence gives a geometric measurement of the topological invariant.

2.2 Persistent similarity

The results from the persistent homology analysis can be represented as following,

$$\{L_{k,j} = [a_{k,j}, b_{k,j}] | k = 0, 1, 2; j = 1, 2, 3, \dots, N_k\}, \quad (8)$$

where parameter k is the dimension of Betti number β_k , parameter j indicates the j -th homology generator and N_k is the number of β_k generator.

Further, I define the sets of barcodes in the k -th dimension,

$$L_k = \{L_{k,j}, j = 1, 2, 3, \dots, N_k\}, \quad k = 0, 1, 2.$$

To visualize the persistent homology results, I use the barcode plot as illustrated in Figure 3 (b). For fullerene C_{44} barcodes, the length of β_0 bars is the atom bond length. The number of β_0 bars are the total number of atoms in the molecular. Further, the pentagon and hexagon ring structures are represented by β_1 bars. The cavity or cage structure of fullerene C_{44} is captured in β_2 bars. These basic chemical implications of the barcodes are very consistent. Moreover, it should be noticed that there is no general way of defining the sequence of the barcodes. I simply define the sequence by birth times of bars.

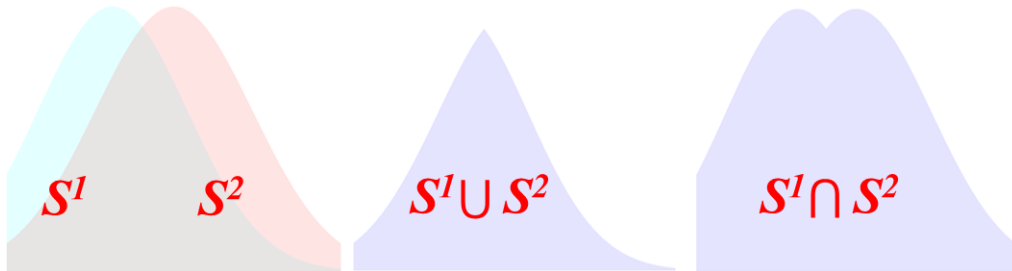


Figure 4: To define persistent similarity from persistent functions. Capitals S^1 and S^2 represent regions under two persistent functions. The persistent similarity P is defined to be the quotient between the intersect area and the union area, i.e., $P = \frac{\int S^1 \cap S^2}{\int S^1 \cup S^2}$

Persistent Betti function (PBF) Based on the barcode, I can build up various model to further explore the biomolecular structure, flexibility, function and dynamics.^{49,54} Among them, persistent Betti function is defined as,

$$f(x; L_k) = \sum_j w_{k,j} e^{-\left(\frac{x - \frac{b_{k,j} + a_{k,j}}{2}}{\sigma(b_{k,j} - a_{k,j})}\right)^\kappa}, \quad \kappa > 0; k = 0, 1, 2. \quad (9)$$

where $w_{k,j}$ is the weight function for the j -th barcode of β_k . Parameter σ is the resolution parameter. It should be noticed that even though there is no meaningful sequence arrangement for barcodes, barcodes derived from the molecules are highly organized. Each bar or each type of bars has its unique structural, physical and chemical implication. With this consideration, I can assign or define a weight value $w_{k,j}$ to each bar or each type of bars. Normally, the weight function and resolution parameter are all chosen as 1, i.e., $\sigma = 1$ and $w_{k,j} = 1$ for all k and j .

More interestingly, PBF provides a unique transformation of persistent barcodes into 1D continuous functions. There is a strict one-to-one correlation between barcodes and PBFs. In this way, any complicated biomolecular structures can be uniquely represented by three 1D PBFs, which dramatically reduced the dimensionality and complexity.

Persistent similarity For two different biomolecular structures denoted as F_1 and F_2 , if their PBFs are $f_1(x; L_k)$ and $f_2(x; L_k)$ and the regions below the two functions is defined as $S_k^1 = \{(x, y) | 0 \leq y(x) \leq f_1(x; L_k); 0 \leq x \leq r_f\}$ and $S_k^2 = \{(x, y) | 0 \leq y(x) \leq f_2(x; L_k); 0 \leq x \leq r_f\}$, the persistent similarity can be defined as

$$P_k(F_1, F_2) = \frac{\int S_k^1 \cap S_k^2}{\int S_k^1 \cup S_k^2}, \quad k = 0, 1, 2. \quad (10)$$

Here r_f is the filtration size. A suitable filtration size is not unique. Usually, it is chosen as the smallest value, after which the filtration generates no significant topological properties.

The above definition of persistent similarity is equivalent to,

$$P_k(F_1, F_2) = \frac{\int \min\{f_1(x; L_k), f_2(x; L_k)\}}{\int \max\{f_1(x; L_k), f_2(x; L_k)\}}, \quad k = 0, 1, 2. \quad (11)$$

Some structures may not have certain significant topological properties. For instance, small molecules may not have β_1 barcodes. In this situation, if it is compared with other molecules with β_1 barcodes, the similarity is always zero, no matter how many or how long the β_1 barcodes in the other structures. This ambiguity brings trouble in structure comparison. To overcome this problem, I introduce a pseudo-barcode into the PBFs and define a new PBF as,

$$f^{pseudo}(x; L_k) = w_{k,0} + \sum_j w_{k,j} e^{-\left(\frac{x - \frac{b_{k,j} + a_{k,j}}{2}}{\sigma(b_{k,j} - a_{k,j})}\right)^\kappa}, \quad \kappa > 0; k = 0, 1, 2. \quad (12)$$

Essentially, a small weight value $w_{k,0}$ is introduced to avoid the situation when PBF is zero function. In this way, I can reduce the ambiguity.

2.3 Multiscale persistent similarity

Biomolecular data are usually highly complicated and essentially multiscale. To overcome this challenge, I have proposed a multiresolution/multiscale persistent homology.⁵⁶ The essential idea is to match the scale of interest with appropriate resolution in the topological analysis. Simply speaking, a resolution parameter is introduced into my multiscale rigidity function, and by turning this parameter, I can focus my topological analysis on any interesting scales. The multiscale rigidity function, which is derived from flexibility and rigidity index (FRI) method,^{34,36-38,50,51} is key to the multiscale persistent homology. By using this function, I can convert a discrete point cloud data into a series of continuous density functions. The conversion is realized by using a kernel function with a resolution or scale parameter. And this special parameter enables us to facilitate a multiscale analysis of complex data. More details will be discussed below.

Multiscale rigidity function For a data set with a total N entries, which can be physical elements like atoms, residues and domains or data components like points, pixels and voxels, if one assumes their generalized coordinates are $\mathbf{r}_1, \mathbf{r}_2, \dots, \mathbf{r}_N$, a multiscale rigidity function of the data can be expressed as,

$$\mu(\mathbf{r}, \eta) = \sum_j^N w_j \Phi(\|\mathbf{r} - \mathbf{r}_j\|; \eta) \quad (13)$$

where w_j is a weight, which usually is chosen as the atomic number, for example, its value is 6 for Carbon atom and 8 for Oxygen atom. The parameter η is the resolution or scale parameter. The function $\Phi(\|\mathbf{r} - \mathbf{r}_j\|; \eta)$ is a kernel function. Commonly used kernel functions are generalized exponential functions,

$$\Phi(\|\mathbf{r} - \mathbf{r}_j\|; \eta, \kappa) = e^{-(\|\mathbf{r} - \mathbf{r}_j\|/\eta)^\kappa}, \quad \kappa > 0 \quad (14)$$

or generalized Lorentz functions,

$$\Phi(\|\mathbf{r} - \mathbf{r}_j\|; \eta, v) = \frac{1}{1 + (\|\mathbf{r} - \mathbf{r}_j\|/\eta)^v}, \quad v > 0. \quad (15)$$

It can be noticed that the larger the η value, the lower the resolution is. A multiscale geometric model can be naturally derived from my multiscale rigidity functions. An example is given in Section 3 Case 4.

Multiscale persistent homology Based on the multiscale rigidity function, I have proposed multiscale persistent homology.^{56,57} In this model, I linearly rescale all the rigidity function values to the region $[0, 1]$ using formula

$$\mu^s(\mathbf{r}, \eta) = 1.0 - \frac{\mu(\mathbf{r}, \eta)}{\mu_{\max}(\eta)}. \quad (16)$$

Here $\mu(\mathbf{r}, \eta)$ and $\mu^s(\mathbf{r}, \eta)$ are the original and normalized rigidity function, and $\mu_{\max}(\eta)$ is the maximum value of the original rigidity function.

I can perform the persistent homology analysis on the rescale rigidity functions. For density data, the filtration parameter is chosen as the isovalue or isosurface value. To be more specific, for each density isovalue, I can generate a molecular surface. With the continuous variation of this value, a series of molecular surfaces are generated. Molecular surfaces are topological spaces and their homology information can be calculated from Morse theory.⁵⁹ Based on these surfaces, Morse complexes are generated and form a nested sequences. In this way, persistent homology analysis can be employed.^{20,31,32}

Multiscale persistent similarity A series of barcodes from various scales are generated in the multiscale persistent homology and can be represented as following,

$$\{L_{k,j}(\eta) = [a_{k,j}(\eta), b_{k,j}(\eta)] | k = 0, 1, 2; j = 1, 2, 3, \dots, N_k(\eta)\}. \quad (17)$$

Similar to the previous definition, parameter k is the dimension of Betti number β_k , parameter j indicates the j -th barcode and N_k is the number of β_k barcodes. And the sets of barcodes in the k -th dimension is represented as,

$$L_k(\eta) = \{L_{k,j}(\eta), j = 1, 2, 3, \dots, N_k(\eta)\}, \quad k = 0, 1, 2$$

Further the multiscale persistent Betti function is represented as,

$$f(x; L_k(\eta)) = \sum_j w_{k,j}(\eta) e^{-\left(\frac{x - \frac{b_{k,j}(\eta) + a_{k,j}(\eta)}{2}}{\sigma(\eta)(b_{k,j}(\eta) - a_{k,j}(\eta))}\right)^\kappa}, \quad \kappa > 0, k = 0, 1, 2. \quad (18)$$

Again $w_{k,j}(\eta)$ is the weight function for the j -th barcode of β_k . Parameter $\sigma(\eta)$ is the resolution or scale parameter.

In this same way, the multiscale persistent similarity between structures $F_1(\eta)$ and $F_2(\eta)$ can be defined as

$$P_k(F_1(\eta), F_2(\eta)) = \frac{\int \min\{f_1(x; L_k(\eta)), f_2(x; L_k(\eta))\}}{\int \max\{f_1(x; L_k(\eta)), f_2(x; L_k(\eta))\}}, \quad k = 0, 1, 2. \quad (19)$$

The multiscale persistent similarity enable us to compare the structure properties from various scales.

3 Results and discussion

In this section, I validate my persistent similarity method using four different cases. In the first case, I consider two similar nucleotide kinases 1AKY and 1GKY. I calculate their persistent similarities for both all-atom-without-hydrogen model and C_α coarse-grained model. The calculated persistent similarities are in the middle range, indicating some potential similarities between two structures. In the second cases, a series of structures of protein 2KIX from NMR experiment are considered. These configurations are highly consistent with only small thermal fluctuations. The persistent similarities for both β_0 and β_1 are of large values, indicating a strong similarity between all the frames. The third cases is devoted to the validation of multiscale persistent similarity. The steered molecular dynamic simulation results of protein Titin are analyzed from two different scales. I find that even though structurally, four extracted frames differ greatly, they local scale properties bear great similarities, meaning local structures have no significant changes in the simulation. Further, I calculate the persistent similarities based on global scale models, a dramatic reduction of similarity values are observe, which is highly consistent with the general unfolding process. The last case is employed for the study of fullerene C_{44} isomers. Since the total curvature energy is highly related to the longest β_2 barcode, the persistent similarity is then defined only on this particular barcode by using the special weight parameters. I establish a linear relation between persistent similarities and total curvature energy differences. More importantly, I find that this linear relation is particularly strong when I use extreme structures for comparison. To void confusion, in all four cases except the last one, the weight function and resolution parameter in the PBF are all chosen as 1, i.e., $\sigma = 1$ and $w_{k,j} = 1$ for all k and j .

3.1 Case 1: Two similar nucleotide kinases

In the first case, I consider two nucleotide kinases (1AKY and 1GKY) used in structural alignment.¹⁸ Two structure description, i.e., all-atom-without-hydrogen model and C_α coarse-grained model, are used for persistent similarity evaluation. Figure 5 illustrates the structure properties of these two proteins. It can be seen that these two structures do share some similar structure components, like the α -helix on the left boundary regions and the β -sheets in the middle regions.

To have a more quantitatively understanding of the structural similarity, I generate the barcodes for both structures in both representations. Figure 6 (a) and (b) are barcodes for all-atom-without-hydrogen model of 1AKY and 1GKY, respectively. As stated above, the length of short β_0 bars represents atomic bond length. And the number of β_0 bars is the number of atoms in the system. In this way, from β_0 bars, chemical components of the structure can be understood. More chemical implications can be learned from β_1 bars. Previously, I have found that, short β_1 bars located in local region around 2.0 Å represent pentagon and hexagon rings in aromatic residues.^{53,54} Particularly, the hexagon rings can further manifest themselves in local β_2 bars. The global structure properties captured by β_1 bars appear much later in the filtration. For

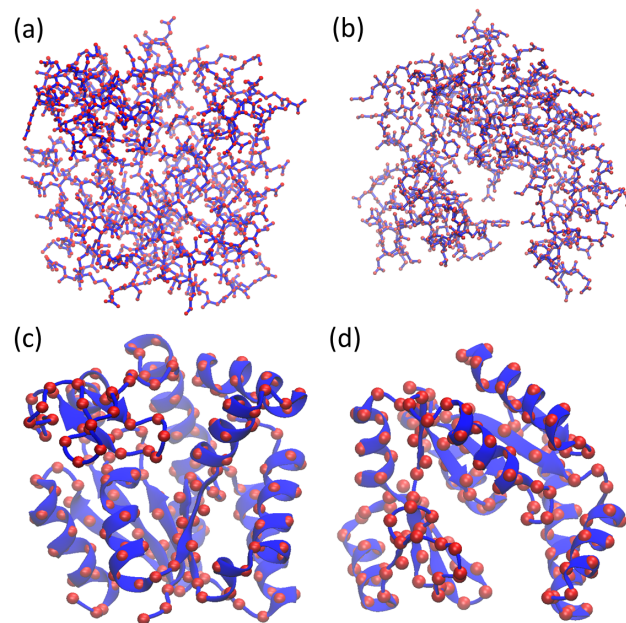


Figure 5: The biomolecular structures of Kinase proteins 1AKY and 1GKY. Two different representations are employed, i.e., all-atom-without-hydrogen model and C_α coarse-grained model. (a) and (b) are all-atom except hydrogen models of 1AKY and 1GKY, respectively. (c) and (d) are C_α coarse-grained model of 1AKY and 1GKY, respectively.

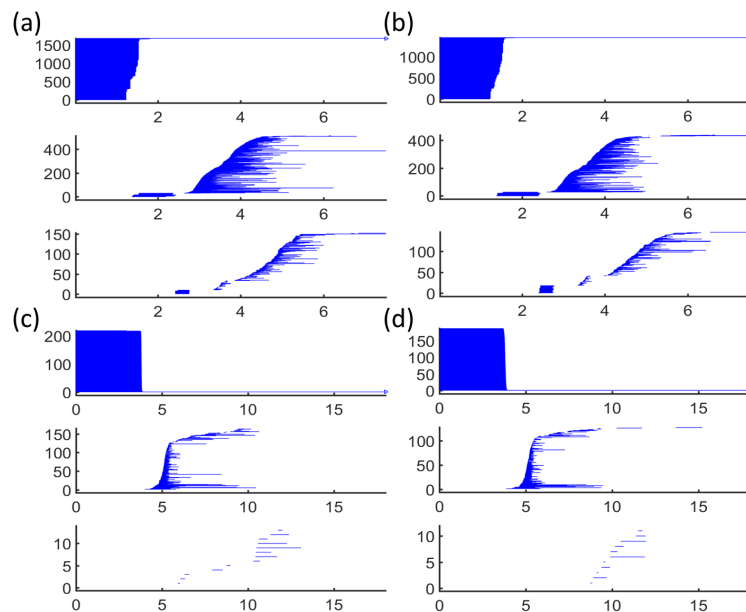


Figure 6: Persistent barcodes for Kinase proteins 1AKY and 1GKY in different representations. (a) and (b) are barcode representations for all-atom without hydrogen models of 1AKY and 1GKY, respectively. (c) and (d) are barcode representations of C_α coarse-grained model of 1AKY and 1GKY, respectively.

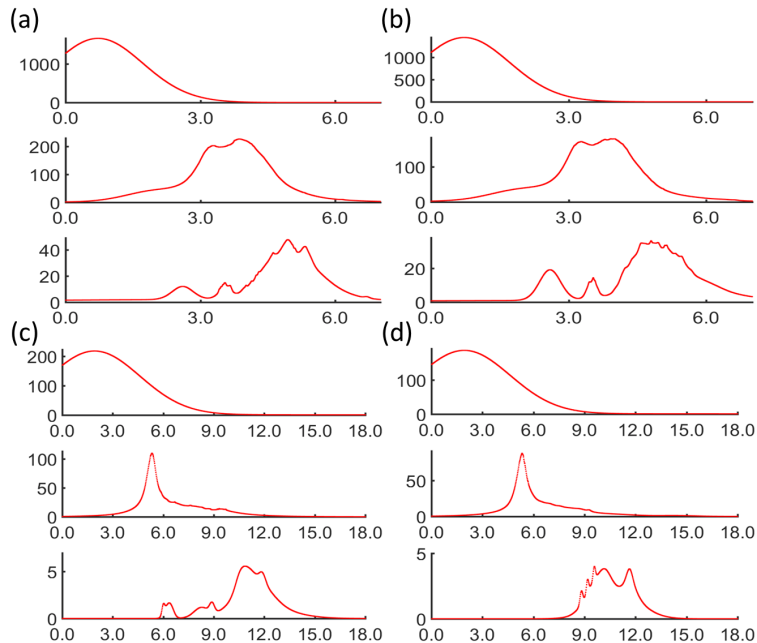


Figure 7: PBFs for Kinase proteins 1AKY and 1GKY in different representations. (a) and (b) are PBFs derived from all-atom-without-hydrogen models of 1AKY and 1GKY, respectively. (c) and (d) are PBFs derived from C_α coarse-grained model of 1AKY and 1GKY, respectively. The persistence similarities between (a) and (b) are 0.860, 0.819, 0.795 for β_0 , β_1 and β_2 , respectively. The persistence similarities between (c) and (d) are 0.857, 0.770, 0.485 for β_0 , β_1 and β_2 , respectively.

all-atom-without-hydrogen model, there is clear separation of local and global type of β_1 bars in both β_1 and β_2 barcodes.

Figure 6 (c) and (d) are barcodes for C_α coarse-grained modeling of 1AKY and 1GKY, respectively. One can see that the length of all short β_0 bars are around 3.8 Å, i.e., the distance between the two adjacent C_α atoms. More over, all three types of barcodes are dramatically reduced. Particularly the β_2 barcodes.

With these barcode results, I can generate the persistent Betti functions. Figure 7 illustrates the basic pattern of PBFs for two proteins in the same sequence as Figure 5 and 6. It can be seen that PBFs are simply one-dimensional functions, which can be easily compared with each other. For all-atom-without-hydrogen models, the persistent similarities are 0.860, 0.819, 0.795 for β_0 , β_1 and β_2 , respectively. For C_α coarse-grained model, the persistence similarities are 0.857, 0.770, 0.485 for β_0 , β_1 and β_2 , respectively. However, in coarse-grained model, there are only a few β_2 barcodes. And many of these bars are extremely short, meaning they are transient state with no topological significance. Therefore, in C_α coarse-grained models, I only consider the β_0 and β_1 persistent similarity.

3.2 Case 2: NMR configurations

In the second case, I consider a NMR solution structure of M-crystallin in calcium free form (PDB ID: 2KIX). There are totally 20 frames in this data. All these configurations are very similar to each other with only small variations due to thermal fluctuation. To quantitatively measure the structure similarity, I consider the C_α coarse-grained representation as illustrated in Figure 8. It should be noticed that I only demonstrate 10 configurations out of 20.

I further perform the persistent homology analysis on these configurations. The persistent similarity is illustrated in Figure 9. More specifically, Figure 9 (a) and (b) are persistent similarity for β_0 and β_1 , respectively. It can be seen that all persistent similarity values are very large. Particularly for β_0 , the values are all around 1.000. For β_1 , the smallest persistent similarity among these twenty configurations is 0.802.

By the comparison of the persistent similarity values between Case 1 and Case 2, one can see that the persistent similarity gives a very reasonable evaluation of the structure similarity. For structures with same

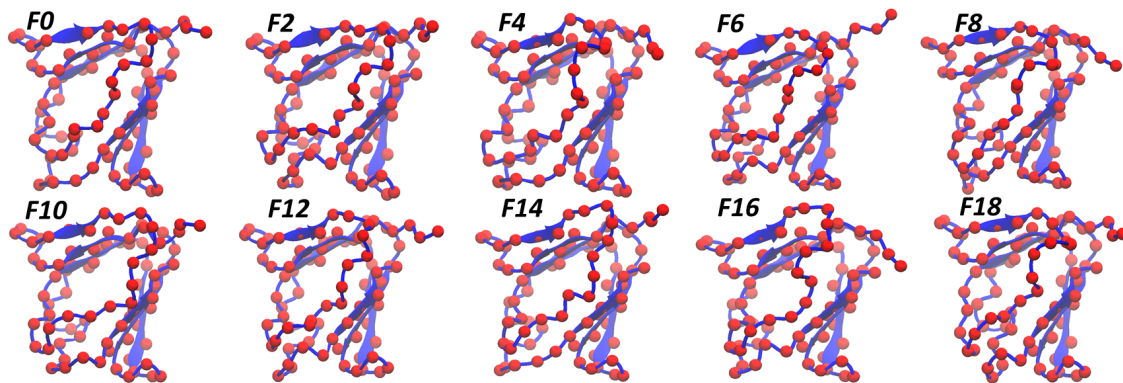


Figure 8: The C_α coarse-grained representations of protein 2KIX. There are totally twenty configurations (denoted as $F1$ to $F20$) in this pdb data generated from NMR. I take ten different configurations among them. It can be seen that they all have very similar structures.

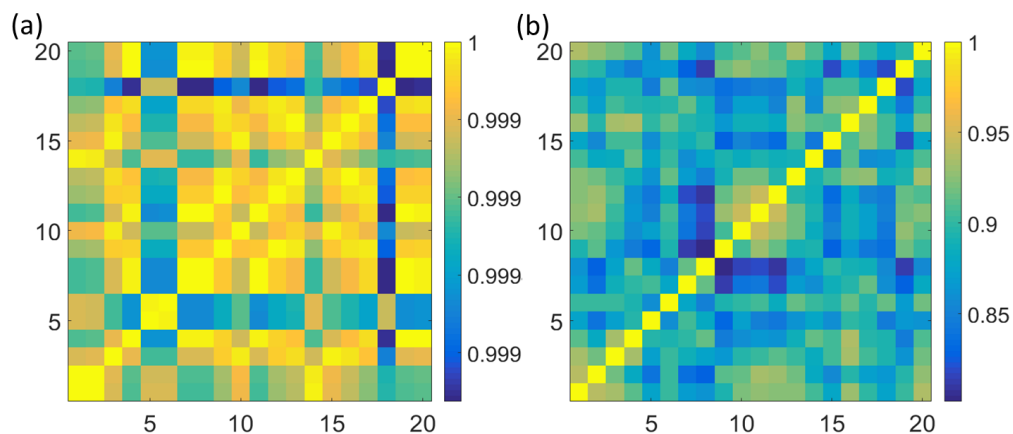


Figure 9: The persistent similarities between twenty different NMR configurations of protein 2KIX. (a) Betti-0 persistent similarities. (b) Betti-1 persistent similarities. It can be seen that Betti-0 persistent similarities are very large and all closed to 1.0. Betti-1 persistent similarities are also relatively high.

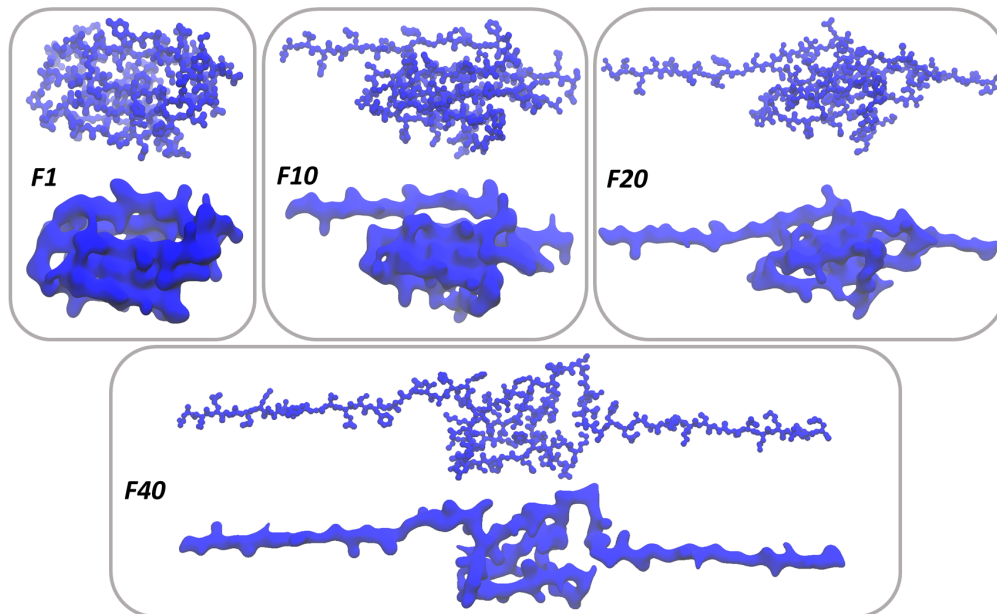


Figure 10: The Titin protein structures derived from steered dynamic simulations. There are totally 89 frames extracted from the simulation. I choose only the frames 1, 10, 20 and 40, denoted as $F1$, $F10$, $F20$ and $F40$, respectively. Two different scale parameters are used, i.e., $\sigma = 0.6 \text{ \AA}$ and 2.0\AA , in the upper and lower figures, respectively.

chemical components, the β_0 persistent homology is all around 0.999, indicating the equivalent structure elements. This is also consistent with chemical implications of β_0 bars. Further, the β_1 persistent similarities for 2K1X structures are all larger the similarity between 1AKY and 1GKY. This is also reasonable from the observations, as 2K1X structures show a clear consistence between each other.

3.3 Case 3: Steered dynamic simulation

In third case, I consider a classic steered molecular dynamic simulation, i.e., Titin I91. The simulation data are directly taken from the VMD timeline tutorial files from <http://www.ks.uiuc.edu/Training/Tutorials/science/timeline/timeline-tutorial-files/>. Four out of eighty-seven frames are picked out for similarity analysis, including frame 1, 10, 20 and 40 (denoted as $F1$ to $F40$). Figure 10 illustrates the multiscale rigidity functions for these four configurations. I choose the generalized exponential kernels as in Eq.14, with parameter $\kappa = 2$ and two different resolution values, i.e., $\sigma = 0.6 \text{ \AA}$ and 2.0 \AA . The density data is generate with the voxel size of 0.3 \AA .

Figure 10 demonstrates the structures of the four frames in two different resolution. The pictures on the upper parts are for resolution value $\sigma = 0.6 \text{ \AA}$ and low parts for $\sigma = 2.0 \text{ \AA}$. The extension process goes from $F1$ to $F40$ and Titin structure is gradually unfolded accordingly. Since different resolution results in density data in different scales, it enables us to observe variations of structure properties from various scales.

Figure 11 illustrates the barcodes for different configurations. Similar to Figure 10, the upper figures indicated as (a) are for resolution value $\sigma = 0.6 \text{ \AA}$ and low figures indicated as (b) are for $\sigma = 2.0 \text{ \AA}$. It can be seen that, barcodes are much more consistent among four configurations in lower resolution. The barcode lengths, total numbers, and basic patterns show great similarity. In contrast, when resolution enlarges to $\sigma = 2.0 \text{ \AA}$, I begin to observe more variations, particularly in β_1 , its total number keeps decreasing as the structure unfolds.

To have a more quantitative comparison, I calculate the persistent similarity between the first frame and the other three. When $\sigma = 0.6 \text{ \AA}$, I have $P(F1, F10) = (0.940, 0.915)$, $P(F1, F20) = (0.915, 0.924)$ and $P(F1, F40) = (0.967, 0.975)$. When $\sigma = 2.0 \text{ \AA}$, I have $P(F1, F10) = (0.832, 0.822)$, $P(F1, F20) = (0.828, 0.695)$ and $P(F1, F40) = (0.573, 0.413)$. Previously I found that for higher resolution ($\sigma = 0.6 \text{ \AA}$), β_0 shows atomic information, longer bars represent atoms with larger atomic number and shorter bars are

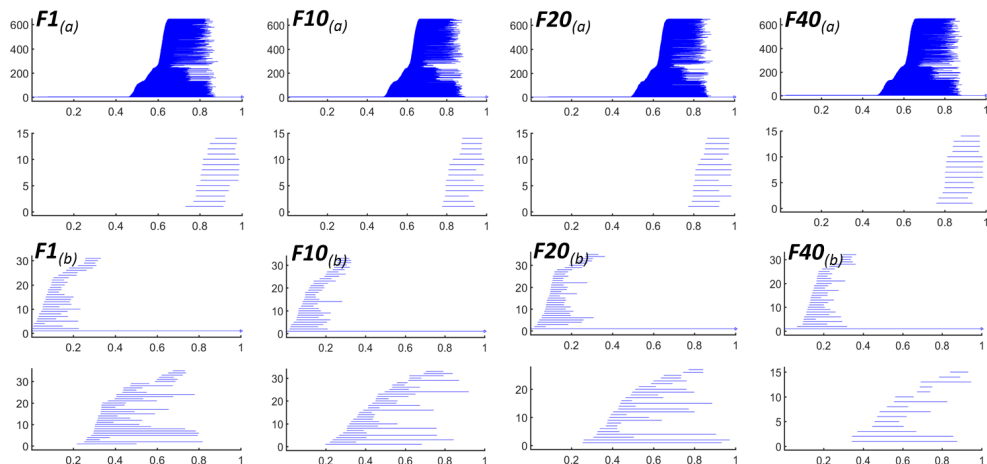


Figure 11: Persistent barcodes for the four configurations in Figure 10.

the inverse.^{56,57} For β_1 , it captures the pentagon and hexagon rings in the aromatic residues. Since atomic information and residues are unchanged during the unfolding process, one will expect a higher persistent similarity in higher resolution structure density data. However, when resolution becomes lower, the fine detailed structure properties are gradually faded away, leaving only the global types of properties. In this case, variations in the folding process should be best represented by the global properties with a lower resolution. My persistent similarity results again confirm my analysis. For higher resolution situation, persistent similarities are very high with values larger than 0.91 for all cases. In lower resolution cases, I find a much smaller similarities, particularly for β_1 . And the values are systematically decreasing, indicating a gradual derivation from the original structure.

It is worth mentioning that even though I have relatively large persistent similarities for higher resolution cases, their persistent similarity is not exactly equal to 1.0 (or just little variation from 1.0). Theoretically, I should have identical β_0 and β_1 persistent similarity values as the β_0 persistent similarity in Case 2. However, due to computational constraints, I only afford to use voxel size of 0.3 Å. In this way, the highest rigidity values for frame 1, 10, 20 and 40 are 15.01, 15.53, 15.03 and 15.30, respectively. This variations induce inconsistency in the normalized rigidity function and further into the barcode results. The voxel size will also have some influence on the results from lower resolution situations.

3.4 Case 4: Fullerene C_{44} isomers

In the last cases, I consider the fullerene C_{44} isomers and its total curvature energies. The fullerene C_{44} isomers structure and energy data can be downloaded from <http://www.nanotube.msu.edu/fullerene/fullerene.php?C=44>. To have a general idea how their structures look like, eight isomer structures are specially chosen and illustrated in Figure 12. Among them, four isomers with the largest total curvature energies are shown in the upper figures. From the large energies to small ones, their indexes are 2, 3, 35 and 1, respectively. Four isomer structures with the smallest total curvature energies are depicted in the lower figures. Again from the large energies to small ones, their indexes are 69, 72, 75 and 89, respectively.

It is found that the isomer total curvature energy is highly related to the regularity of isomer cage structure. The longest β_2 barcode, representing the cage size, has been found to be linearly related to these energies.⁴⁸ In this case, I further explore the relation of structure similarities and total curvature energy differences. To remove the irrelevant topological properties, in my PBFs, only the weight for the longest β_2 barcode is chosen as 1.0 with all the others set as 0.0. And I only consider the β_2 PBFs. First, I compare the similarity between isomer C_{44} -89 and all isomers, and its relation with the total curvature energies. Figure 13 (a) and (b) illustrate the results of energies and similarities, respectively. It can be seen that there is inverse relation between them. Actually, the Pearson correlation coefficient (PCC) between them are -0.952, which is better than distance filtration⁴⁸ and density filtration results,⁴⁷ and as good as correlation matrix results.⁴⁸

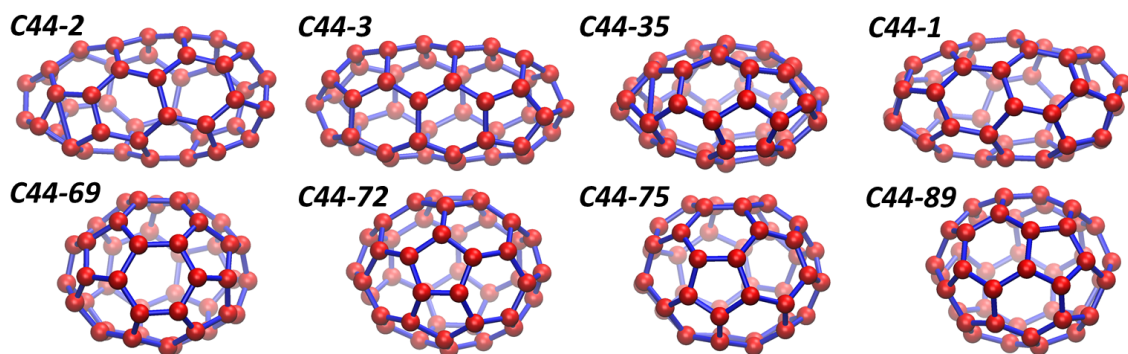


Figure 12: The illustration of eight different fullerene C_{44} isomer structures. Fullerene C_{44} has totally 89 isomers. These isomers have different total curvature energies. I have demonstrated four isomer structures with the largest total curvature energies in the upper figures. From the large energies to small ones, their indexes are 2, 3, 35 and 1, respectively. I have illustrated four isomer structures with the smallest total curvature energies in the lower figures. Again from the large energies to small ones, their indexes are 69, 72, 75 and 89, respectively.

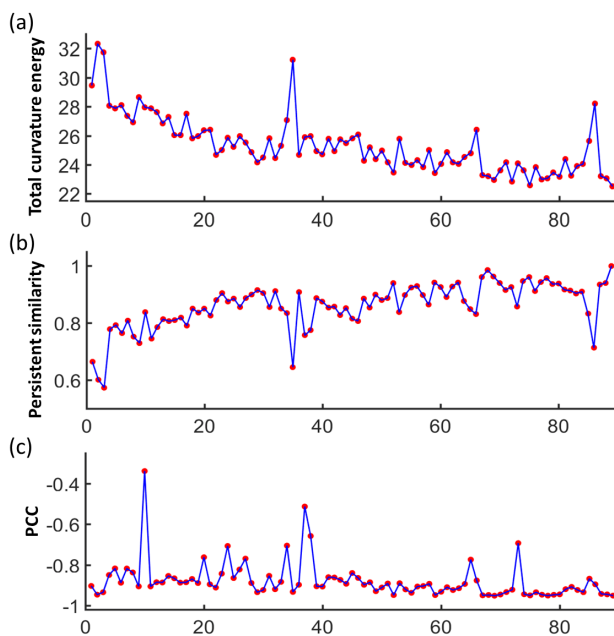


Figure 13: The comparison between total curvature energies and persistent similarities of 89 fullerene C_{44} isomers. (a) is the total curvature energies of 89 fullerene C_{44} isomers. (b) is the persistent similarities between all isomers with the isomer 89. (c) The Pearson correlation coefficient (PCC) of persistent similarities and curvature energy differences. For each isomer, I calculate its persistent similarities with all isomers including itself, then I compare these similarity values with the corresponding curvature energy differences (absolute value) to get PCC values.

Further, I change the reference isomer form C_{44-89} to others and recalculate the PCC between persistent similarity values and curvature energy differences. To avoid confusion, the energy differences are taken as the absolute difference value and are always positive. The PCCs are illustrated in Figure 13 (c). It can be seen that most of the PCCs are larger than 0.80. More interesting, using the isomers with more extreme curvature energies as the reference gives higher PCCs. In contrast, if the reference isomer is chosen from the ones with intermediate curvature energies, there will be a small PCC value. This is reasonable because similarity measures the “absolute” difference. Therefore, one should always go to the extreme cases for similarity evaluation so that it can bring out more intrinsic differences. It should be noticed that a Wasserstein metric based similarities may have the potential to avoid this problem. However, this falls out of the scope of the current paper and will be further explored later.

4 Conclusion remarks

In this paper, I introduce a persistent similarity model for structure comparison. Based on the persistent homology analysis, the persistent similarity can deliver a quantitative comparison of the intrinsic topological properties. In this model, a persistent Betti function is proposed to represent the barcodes from the persistent homology analysis into a series of one-dimensional functions. The similarity is defined as the ratio of the sizes of intersect areas and union areas from these functions. Further, in order to avoid the ambiguity of comparing structures with no significant topological properties, a pseudo-barcode is introduced. Moreover, multiscale persistent similarity is also introduced to facilitate the comparison of structure properties in different scales. The persistent similarity method is validated with several test examples. It is found that the persistent similarity can be used to describe the intrinsic similarities and differences between the structures very well.

The proposed persistent similarity has several unique properties. Firstly, with the representation of structures in PBFs, the comparison between various structure can be done very efficiently. In my persistent similarity, any complicated biomolecular structure can be reduced to several simple 1D PBFs for comparison. Their similarity is then defined as the quotient between sizes of intersect areas and union areas below two correspondingly PBFs. Secondly, the multiscale persistent similarity enables an objective-oriented comparison. Through the multiscale rigidity function, a multiscale biomolecular representation is achieved and naturally induces a multiscale persistent similarity. Since my multiscale representation can be adjusted to any resolutions, the associated persistent similarity can be used to compare structures in any particular scale of interest. Thirdly, a pseudo-barcode is introduced to deliver a more precise comparison in the special situation when structures have no significant topological properties.

In future, I will explore the application of persistent similarity in protein structure classification⁴² and compare with existing methods to demonstrate its full potential. Further, I will consider Wasserstein metric as a new similarity measurement.

Acknowledgments

This work was supported by NTU [sug-m4081842.110](#) and MOE AcRF Tier 1 M401110000.

References

- [1] Dionysus: the persistent homology software. Software available at <http://www.mrzv.org/software/dionysus>.
- [2] U. Bauer, M. Kerber, and J. Reininghaus. Distributed computation of persistent homology. *Proceedings of the Sixteenth Workshop on Algorithm Engineering and Experiments (ALENEX)*, 2014.
- [3] P. Bendich, H. Edelsbrunner, and M. Kerber. Computing robustness and persistence for images. *IEEE Transactions on Visualization and Computer Graphics*, 16:1251–1260, 2010.
- [4] J. Binchi, E. Merelli, M. Rucco, G. Petri, and F. Vaccarino. jholes: A tool for understanding biological complex networks via clique weight rank persistent homology. *Electronic Notes in Theoretical Computer Science*, 306:5–18, 2014.
- [5] P. Bubenik. Statistical topological data analysis using persistence landscapes. *Journal of Machine Learning Research*, 16(1):77–102, 2015.

- [6] P. Bubenik and P. T. Kim. A statistical approach to persistent homology. *Homology, Homotopy and Applications*, 19:337–362, 2007.
- [7] G. Carlsson. Topology and data. *Am. Math. Soc.*, 46(2):255–308, 2009.
- [8] G. Carlsson, T. Ishkhanov, V. Silva, and A. Zomorodian. On the local behavior of spaces of natural images. *International Journal of Computer Vision*, 76(1):1–12, 2008.
- [9] T. K. Dey, K. Y. Li, J. Sun, and C. S. David. Computing geometry aware handle and tunnel loops in 3d models. *ACM Trans. Graph.*, 27, 2008.
- [10] T. K. Dey and Y. S. Wang. Reeb graphs: Approximation and persistence. *Discrete and Computational Geometry*, 49(1):46–73, 2013.
- [11] B. Di Fabio and C. Landi. A Mayer-Vietoris formula for persistent homology with an application to shape recognition in the presence of occlusions. *Foundations of Computational Mathematics*, 11:499–527, 2011.
- [12] H. Edelsbrunner and J. Harer. *Computational topology: an introduction*. American Mathematical Soc., 2010.
- [13] H. Edelsbrunner, D. Letscher, and A. Zomorodian. Topological persistence and simplification. *Discrete Comput. Geom.*, 28:511–533, 2002.
- [14] S. Erten, G. Bebek, and M. Koyutürk. Vavien: an algorithm for prioritizing candidate disease genes based on topological similarity of proteins in interaction networks. *Journal of computational biology*, 18(11):1561–1574, 2011.
- [15] C. J. Feinauer, A. Hofmann, S. Goldt, L. Liu, G. Mate, and D. W. Heermann. Zinc finger proteins and the 3D organization of chromosomes. *Advances in Protein Chemistry and Structural Biology*, 90:67–117, 2013.
- [16] P. Frosini and C. Landi. Persistent Betti numbers for a noise tolerant shape-based approach to image retrieval. *Pattern Recognition Letters*, 34(8):863–872, 2013.
- [17] M. Gameiro, Y. Hiraoka, S. Izumi, M. Kramar, K. Mischaikow, and V. Nanda. Topological measurement of protein compressibility via persistence diagrams. *preprint*, 2013.
- [18] J. C. Gelly, A. P. Joseph, N. Srinivasan, and A. G. de Brevern. iPBA: a tool for protein structure comparison using sequence alignment strategies. *Nucleic acids research*, 39(suppl 2):W18–W23, 2011.
- [19] R. Ghrist. Barcodes: the persistent topology of data. *Bulletin of the American Mathematical Society*, 45(1):61–75, 2008.
- [20] Shaun Harker, Konstantin Mischaikow, Marian Mrozek, Vidit N, Hubert Wagner, and Mateusz Juda. The efficiency of a homology algorithm based on discrete morse theory and coreductions. *Proceeding of the 3rd International Workshop on Computational Topology in Image Context, Image A*, pages 41–47, 2010.
- [21] D. Horak, S Maletic, and M. Rajkovic. Persistent homology of complex networks. *Journal of Statistical Mechanics: Theory and Experiment*, 2009(03):P03034, 2009.
- [22] T. Kaczynski, K. Mischaikow, and M. Mrozek. *Computational homology*. Springer-Verlag, 2004.
- [23] P. M. Kasson, A. Zomorodian, S. Park, N. Singhal, L. J. Guibas, and V. S. Pande. Persistent voids a new structural metric for membrane fusion. *Bioinformatics*, 23:1753–1759, 2007.
- [24] P. Koehl. Protein structure similarities. *Current opinion in structural biology*, 11(3):348–353, 2001.
- [25] H Lee, H. Kang, M. K. Chung, B. Kim, and D. S. Lee. Persistent brain network homology from the perspective of dendrogram. *Medical Imaging, IEEE Transactions on*, 31(12):2267–2277, Dec 2012.

- [26] C. Lei and J. Ruan. A novel link prediction algorithm for reconstructing protein–protein interaction networks by topological similarity. *Bioinformatics*, 29(3):355–364, 2013.
- [27] X. Liu, Z. Xie, and D. Y. Yi. A fast algorithm for constructing topological structure in large data. *Homology, Homotopy and Applications*, 14:221–238, 2012.
- [28] G. Máté and D. W. Heermann. Statistical analysis of protein ensembles. *Frontiers in Physics*, 2:20, 2014.
- [29] G. Máté, A. Hofmann, N. Wenzel, and D. W. Heermann. A topological similarity measure for proteins. *Biochimica et Biophysica Acta (BBA)-Biomembranes*, 1838(4):1180–1190, 2014.
- [30] K. Mischaikow, M Mrozek, J. Reiss, and A. Szymczak. Construction of symbolic dynamics from experimental time series. *Physical Review Letters*, 82:1144–1147, 1999.
- [31] K. Mischaikow and V. Nanda. Morse theory for filtrations and efficient computation of persistent homology. *Discrete and Computational Geometry*, 50(2):330–353, 2013.
- [32] Konstantin Mischaikow and Vidit Nanda. Morse theory for filtrations and efficient computation of persistent homology. *Discrete Comput. Geom.*, 50(2):330–353, 2013.
- [33] Vidit Nanda. Perseus: the persistent homology software. Software available at <http://www.sas.upenn.edu/~vnanda/perseus>.
- [34] D. Nguyen, K. L. Xia, and G. W. Wei. Generalized flexibility-rigidity index. *The Journal of Chemical Physics*, 144(23):234106, 2016.
- [35] P. Niyogi, S. Smale, and S. Weinberger. A topological view of unsupervised learning from noisy data. *SIAM Journal on Computing*, 40:646–663, 2011.
- [36] K. Opron, K. L. Xia, Z. F. Burton, and G. W. Wei. Flexibility-rigidity index for protein-nucleic acid flexibility and fluctuation analysis. *Journal of Computational Chemistry*, 37(14):1283–1295, 2016.
- [37] K. Opron, K. L. Xia, and G. W. Wei. Fast and anisotropic flexibility-rigidity index for protein flexibility and fluctuation analysis. *Journal of Chemical Physics*, 140:234105, 2014.
- [38] K. Opron, K. L. Xia, and G.W. Wei. Communication: Capturing protein multiscale thermal fluctuations. *The Journal of chemical physics*, 142(21):211101, 2015.
- [39] D. Pachauri, C. Hinrichs, M.K. Chung, S.C. Johnson, and V. Singh. Topology-based kernels with application to inference problems in alzheimer’s disease. *Medical Imaging, IEEE Transactions on*, 30(10):1760–1770, Oct 2011.
- [40] B. Rieck, H. Mara, and H. Leitte. Multivariate data analysis using persistence-based filtering and topological signatures. *IEEE Transactions on Visualization and Computer Graphics*, 18:2382–2391, 2012.
- [41] Vanessa Robins. Towards computing homology from finite approximations. In *Topology Proceedings*, volume 24, pages 503–532, 1999.
- [42] P. Røgen and B. Fain. Automatic classification of protein structure by using Gauss integrals. *Proceedings of the National Academy of Sciences*, 100(1):119–124, 2003.
- [43] V. D. Silva and R Ghrist. Blind swarms for coverage in 2-d. In *In Proceedings of Robotics: Science and Systems*, page 01, 2005.
- [44] G. Singh, F. Memoli, T. Ishkhanov, G. Sapiro, G. Carlsson, and D. L. Ringach. Topological analysis of population activity in visual cortex. *Journal of Vision*, 8(8), 2008.
- [45] Andrew Tausz, Mikael Vejdemo-Johansson, and Henry Adams. Javaplex: A research software package for persistent (co)homology. Software available at <http://code.google.com/p/javaplex>, 2011.

- [46] B. Wang, B. Summa, V. Pascucci, and M. Vejdemo-Johansson. Branching and circular features in high dimensional data. *IEEE Transactions on Visualization and Computer Graphics*, 17:1902–1911, 2011.
- [47] B. Wang and G. W. Wei. Object-oriented persistent homology. *Journal of Computational Physics*, 305:276–299, 2016.
- [48] K. L. Xia, X. Feng, Y. Y. Tong, and G. W. Wei. Persistent homology for the quantitative prediction of fullerene stability. *Journal of Computational Chemistry*, 36:408–422, 2015.
- [49] K. L. Xia, Z. M. Li, and L. Mu. Multiscale persistent functions for biomolecular structure characterization. *Bulletin of Mathematical Biology, revised*.
- [50] K. L. Xia, K. Opron, and G. W. Wei. Multiscale multiphysics and multidomain models - Flexibility and Rigidity. *Journal of Chemical Physics*, 139:194109, 2013.
- [51] K. L. Xia, K. Opron, and G. W. Wei. Multiscale Gaussian network model (mGNM) and multiscale anisotropic network model (mANM). *The Journal of chemical physics*, 143(20):204106, 2015.
- [52] K. L. Xia and G. W. Wei. Persistent homology analysis of protein structure, flexibility and folding. *International Journal for Numerical Methods in Biomedical Engineerings*, 30:814–844, 2014.
- [53] K. L. Xia and G. W. Wei. Persistent homology analysis of protein structure, flexibility, and folding. *International journal for numerical methods in biomedical engineering*, 30(8):814–844, 2014.
- [54] K. L. Xia and G. W. Wei. Multidimensional persistence in biomolecular data. *Journal Computational Chemistry*, 36:1502–1520, 2015.
- [55] K. L. Xia and G. W. Wei. Persistent topology for cryo-EM data analysis. *International Journal for Numerical Methods in Biomedical Engineering*, 31:e02719, 2015.
- [56] K. L. Xia, Z. X. Zhao, and G. W. Wei. Multiresolution persistent homology for excessively large biomolecular datasets. *The Journal of chemical physics*, 143(13):134103, 2015.
- [57] K. L. Xia, Z. X. Zhao, and G. W. Wei. Multiresolution topological simplification. *Journal Computational Biology*, 22:1–5, 2015.
- [58] Y. Yao, J. Sun, X. H. Huang, G. R. Bowman, G. Singh, M. Lesnick, L. J. Guibas, V. S. Pande, and G. Carlsson. Topological methods for exploring low-density states in biomolecular folding pathways. *The Journal of Chemical Physics*, 130:144115, 2009.
- [59] A. Zomorodian and G. Carlsson. Computing persistent homology. *Discrete Comput. Geom.*, 33:249–274, 2005.
- [60] A. Zomorodian and G. Carlsson. Localized homology. *Computational Geometry - Theory and Applications*, 41(3):126–148, 2008.